Bioorganic & Medicinal Chemistry 25 (2017) 2156–2166

Contents lists available at ScienceDirect

Bioorganic & Medicinal Chemistry

journal homepage: www.elsevier.com/locate/bmc

Novel pyrrolopyrimidines as Mps1/TTK kinase inhibitors for breast cancer

Yasuro Sugimoto [a], Dwitiya B. Sawant [b], Harold A. Fisk [b], Liguang Mao [a], Chenglong Li [a], Somsundaram Chettiar [a], Pui-Kai Li [a], Michael V. Darby [a], Robert W. Brueggemeier [a,*]

[a] Division of Medicinal Chemistry and Pharmacognosy, College of Pharmacy, The Ohio State University, Columbus, OH 43210, USA
[b] Department of Molecular Genetics, College of Arts & Sciences, The Ohio State University, Columbus, OH 43210, USA

ARTICLE INFO

Article history:
Received 3 November 2016
Revised 10 February 2017
Accepted 12 February 2017
Available online 16 February 2017

Keywords:
Mps-1
TTK
Spindle checkpoint kinases
Centrosome amplification
Pyrrolopyrimidine analogues
Breast cancer

ABSTRACT

New targeted therapy approaches for certain subtypes of breast cancer, such as triple-negative breast cancers and other aggressive phenotypes, are desired. High levels of the mitotic checkpoint kinase Mps1/TTK have correlated with high histologic grade in breast cancer, suggesting a potential new therapeutic target for aggressive breast cancers (BC). Novel small molecules targeting Mps1 were designed by computer assisted docking analyses, and several candidate compounds were synthesized. These compounds were evaluated in anti-proliferative assays of a panel of 15 breast cancer cell lines and further examined for their ability to inhibit a variety of Mps1-dependent biological functions. The results indicate that the lead compounds have strong anti-proliferative potential through Mps1/TTK inhibition in both basal and luminal BC cell lines, exhibiting IC_{50} values ranging from 0.05 to 1.0 μM. In addition, the lead compounds **1** and **13** inhibit Mps1 kinase enzymatic activity with IC_{50} values from 0.356 μM to 0.809 μM, and inhibited Mps1-associated cellular functions such as centrosome duplication and the spindle checkpoint in triple negative breast cancer cells. The most promising analog, compound **13**, significantly decreased tumor growth in nude mice containing Cal-51 triple negative breast cancer cell xenografts. Using drug discovery technologies, computational modeling, medicinal chemistry, cell culture and *in vivo* assays, novel small molecule Mps1/TTK inhibitors have been identified as potential targeted therapies for breast cancers.

1. Introduction

Breast cancer (BC) is a heterogeneous group of tumors which can be subdivided on the basis of histopathological features, genetic alterations, and gene-expression profiles.[1,2] Approximately 50–60% of all breast cancer patients and two-thirds of postmenopausal breast cancer patients have estrogen receptor positive tumors (ER+). Adjuvant hormonal therapy is the primary therapy for ER+ breast cancer. Triple-negative breast cancers (TNBC) are defined by the absence of staining for estrogen receptors, progesterone receptors, and HER2/neu. These tumors have poor clinical outcome and represent a recognized prognostic group characterized by aggressiveness[3] and resistance to available systemic therapy. Approximately 10–25% of all breast cancers in the U.S. are TNBC.

A 2011 study reported a high-throughput RNAi screening of a series of pharmacologically tractable genes followed by comprehensive functional viability assay profiles for a panel in >30 commonly used breast tumor cell models to identify genes critical to the growth of specific breast cancer subtypes.[4] Analysis of these profiles identified a series of novel genetic dependencies and suggested potential new therapeutic targets for aggressive breast cancers. One group of genes identified was mitotic checkpoint kinases, including Mps1/TTK. Other studies in 2011 and 2013 reported that high levels of Mps1 protein has been correlated with high histologic grade in breast cancer, while reducing Mps1 levels in BC cells by RNAi resulted in aberrant mitoses, induction of apoptosis, and decreased ability of BC cells to grow as xenografts in nude mice.[5,6] These studies suggest Mps1 as a potential therapeutic target in aggressive breast cancers.

While the Mps1 gene (monopolar spindle) was first identified in the budding yeast, *Saccharomyces cerevisiase*,[7] its human ortholog [phosphotyrosine-picked threonine kinase/threonine and tyrosine kinase (PYT/TTK)] had been discovered as a dual specificity protein kinase.[8,9] Mps1/TTK regulates cell cycle progression,[10,11] and both mRNA and protein levels of Mps1 are readily detectable in proliferating breast cancer cells, while markedly reduced or absent

* Corresponding author.
E-mail address: Brueggemeier.1@osu.edu (R.W. Brueggemeier).

http://dx.doi.org/10.1016/j.bmc.2017.02.030
0968-0896/

in breast cancer cells with a low proliferative index. Mps1/TTK regulates several processes that are important for genomic integrity such as centrosome duplication,[12–14] DNA damage control,[15] and the spindle assembly checkpoint (SAC),[12] and alterations to Mps1/TTK have been associated with cell transformation and chromosome instability in different tumor models.[16]

As many as 80% of invasive breast tumors have extra centrosomes[17] that generate aberrant mitotic spindles *in situ*,[18] and the appearance of extra centrosomes is an early occurrence in breast tumorigenesis[17] that correlates with aneuploidy in invasive tumors.[17,19] Preventing the degradation of Mps1 is sufficient to cause centrosome re-duplication,[13,14,20] and defects in this control are correlated with centrosome amplification and tumorigenesis.[14,21] Notably, breast cells are particularly sensitive to increases in Mps1/TTK protein levels and, unlike in other cell types, overexpression of wild type Mps1/TTK causes centrosome re-duplication in breast-derived cells.[14] Several centrosome defects have been observed in breast cancer, including centrosome amplification, centrioles of unusual length, and accumulation of phosphorylated forms of Centrin 2 (Cetn2),[19,22,23] an Mps1 substrate whose function and localization at the centrosome are regulated by Mps1 phosphorylation.[24–26]

The role of Mps1 has been most widely studied in the SAC, which ensures proper chromosome segregation by delaying progression through mitosis until chromosomes are all properly aligned. Mps1 accumulates at unattached or misaligned kinetochores[27] where it plays a key role in recruitment of several other checkpoint proteins.[28,29] Also, reports suggest that silencing Mps1/TTK, which has dual roles in checkpoint activation and chromosome alignment, can sensitize cancer cells to sub-lethal doses of paclitaxel, whereas non-tumorigenic cells cannot be sensitized.[30,31]

These observations suggest that pharmacological inhibition of Mps1/TTK may be a promising targeted cancer therapeutic. Several Mps1/TTK inhibitors have been developed in recent years,[32–38] such as Mps1-IN-1, Mps1-IN-3, reversine (originally identified as an Aurora B inhibitor),[39] AZ3146, Mps-BAY1, Mps1-BAY2a, BAY 1217389, MPI-0479605, and CCT251455. In most cases, however, only the SAC function of Mps1 was assayed, or as for Mps1-IN-1, Mps1-BAY1 and Mps1-BAY2a there was no inhibition of centrosome duplication. Current therapies for certain subtypes of breast cancer, such as TNBC and other aggressive phenotypes, rely on standard chemotherapy approaches with significant side effects; therefore, newer targeted therapy approaches are needed. This research focused on designing and developing novel small molecule Mps1/TTK inhibitors as targeted therapies for TNBC and aggressive breast cancers. Such agents are envisioned to replace standard cytotoxic chemotherapies as monotherapy or in combination with current treatment regimens as safe, effective interventions that reduce life-threatening toxicities. In this study we describe two novel small molecule inhibitors of Mps1, Compound **1** and Compound **13**, that inhibit both centrosome duplication and SAC function. Furthermore, Compound **13** attenuates growth of triple negative breast cancer cells in mouse xenografts.

2. Results

2.1. Computational drug design

Using computer assisted docking studies, a series of novel molecules were designed to interact at the Mps1-ATP competitive binding site. A computational study of known chemical scaffolds led us to the design of lead compound **1** (Fig. 1) to explore as Mps1/TTK inhibitors. *In silico* analysis of our unique lead scaffold identified twin hydrogen bonds between our novel chemical scaffold, a pyrrolopyrimidine ring, and the kinase hinge loop, which should impart strong inhibitor binding (Fig. 1). The hydrogen bonds are between carbonyl oxygen of Glu603 and pyrrole nitrogen and between amide of Gly605 and pyrimidine nitrogen. The binding modes are very similar to that of Mps1-IN-1,[33] except that the twin hydrogen bonds are 0.9 kcal/mol stronger due to the substitution of pyridine ring of Mps1-IN-1 to the pyrimidine ring, translating to a 5-fold increase in potency at enzymatic level.

For lead optimization, research focuses on adding fragments into Site 1 to gain potency and selectivity and on replacing fragments at Site 2 to gain potency and improve drug properties (Fig. 1). Site 1 is a particularly attractive site for modifications as this site is not occupied by substituents in current inhibitors. Site 2 affords opportunities for fragment substitutions that will enhance pharmacokinetic parameters. As a result of the computational drug design, compound **1** (Fig. 1) was synthesized as a lead compound for investigation.

2.2. Synthesis of the inhibitors

The synthesis of compounds **1**, **7**, **9** and **13** are shown in Fig. 2. The synthesis began with the known compound 2,4-dichloro-7H-pyrrolo[2,3-*d*]pyrimidine **2**.[40] The N7 position of compound **2** was selectively protected using di-*tert*-butyl dicarbonate to form the carboxylate **3**.[41] Crossing coupling of **3** with 2-(isopropylsulfonyl)aniline afforded **4**. Nucleophilic aromatic substitution with 2-methoxyaniline and 1-(4-amino-3-methoxy)piperidin-4-ol formed compounds **5** and **6**, respectively. Boc-deprotection of **5** and **6** yielded the respective compounds **1** and **7**.

Intermediate **4** was used for the synthesis of compound **9**. Nucleophilic aromatic substitution of **4** with 2-methoxy-4-morpholinoaniline obtained **8**. Boc-deprotection of **8** yielded compound **9**. Finally, cyclohexylamine was reacted with 2,6-dichloropyrrolopyrimidine in presence of a base[42] to form **10**. The N7 position of compound **10** was then protected using di-*tert*-butyl dicarbonate to yield **11**. Aromatic substitution of **11** with 2-methoxy-4-morpholinoaniline followed by boc deprotection afforded compound **13**.

2.3. Drug validation

In vitro evaluation of synthesized molecules included the determination of anti-proliferative effects on breast cancer cell lines, kinase inhibition assays, and functional cell biology studies on centriole assembly and the spindle checkpoint.

2.3.1. Anti-proliferative effects

The synthesized molecules were examined for anti-proliferative effects on numerous breast cancer cell lines, including hormone-responsive cell lines and triple-negative cell lines. The IC_{50} values of compounds **1**, **7**, **9** and **13** ranged from 0.05 to 1.0 μM in several breast cancer cell lines (Table 1). In general, the compounds demonstrated anti-proliferative effects in TNBC basal cells and in luminal breast cancer cell types. Compounds **1** and **13** were also tested in the primary cultures of normal breast epithelial cells; both compounds exhibited no inhibition or incomplete dose-response curves up to 20 μM.

2.3.2. Mps1 kinase inhibition

To determine the efficacy of candidate compounds against Mps1/TTK kinase activity, assays were performed as previously described[24] using recombinant Mps1, Cetn2 (specific substrate), and varying concentrations of the inhibitors. This enzyme assay using Cetn2 exhibits greater sensitivity than using a generic substrate (e.g., MBP). In the enzyme assay, compound **1** inhibits

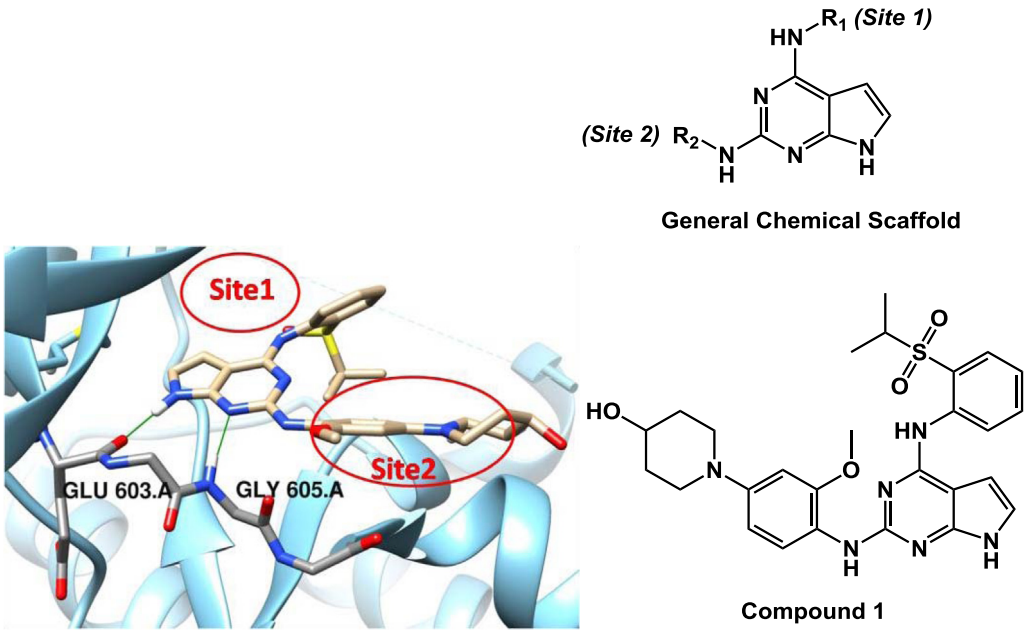

Fig. 1. General chemical scaffold and lead Compound **1** binding to kinase ATP site.

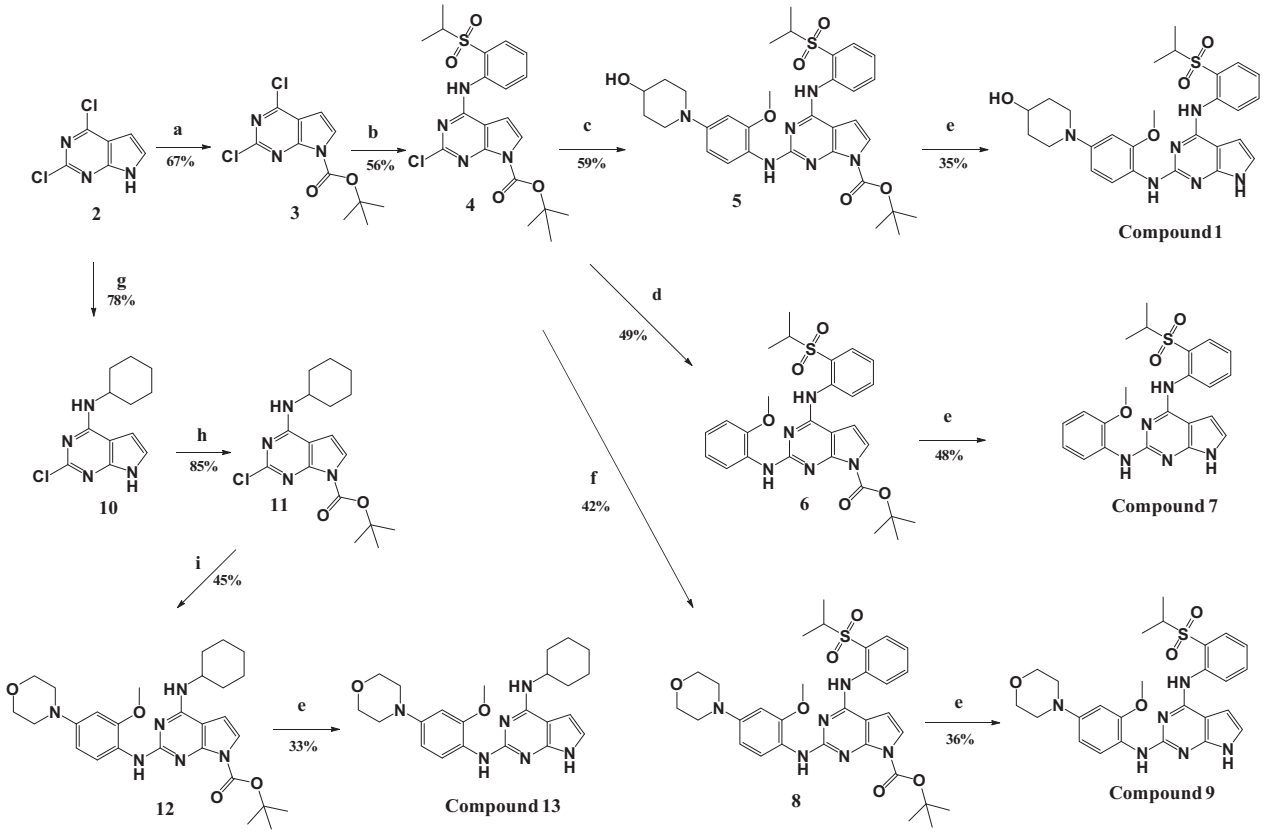

Fig. 2. Syntheses of Compounds **1**, **7**, **9** and **13**. Reagents and conditions: (a) di-*tert*-Butyldicarbonate, DMAP, DIEA, DCM, reflux, 15 min. (b) 2-(Isopropylsulfonyl)aniline, $Pd_2(dba)_3$, XPhos, K_2CO_3, *t*-butanol, 100 °C, 4 h. (c) 1-(4-Amino-3-methoxyphenyl-piperidin-4-ol, $Pd_2(dba)_3$, XPhos, K_2CO_3, *t*-butanol, 100 °C, 6 h. (d) 2-Methoxyaniline, $Pd_2(dba)_3$, XPhos, K_2CO_3, *t*-butanol, 100 °C, 4 h. (c) 1-(4-amino-3-methoxyphenyl)-piperidin-4-ol, $Pd_2(dba)_3$, XPhos, K_2CO_3, *t*-butanol, 100 °C, 6 h. (e) TFA, DCM, rt, 4 h. (f) 2-Methoxy-morpholinoaniline, $Pd_2(dba)_3$, XPhos, K_2CO_3, *t*-butanol, 100 °C, 4 h. (g) Cyclohexylamine, TEA, EtOH, reflux, overnight. (h) di-*tert*-butyldicarbonate, DMAP, DIEA, DCM, reflux, 15 min. (i) 2-methoxy-4-morpholinoaniline, $Pd_2(dba)_3$, XPhos, K_2CO_3, *t*-butanol, 100 °C, 6 h.

in vitro kinase activity of Mps1 with an IC_{50} value of 0.809 μM and compound **13** with an IC_{50} value of 0.356 μM. Compound **7** and compound **9** were less effective, with IC_{50} values of 3.4 and 13.1 μM, respectively. On the other hand, Mps1-IN-1 exhibits an IC_{50} value of 1.7 μM in our assay system. Compound **13** was further evaluated in kinase profiling assays for twenty common kinases

Table 1
IC_{50} determinations of compounds 1, 7, 9, 13, and known inhibitor, Mps1-IN-1, in panel of breast cancer cell lines.

Cell line			IC_{50} ± SEM (μM)				
		BASAL subtype	Cpd 1	Cpd 7	Cpd 9	Cpd 13	Mps1-IN-1
CAL-51	TNBC	Basal	0.23 ± 0.04	1.26 ± 0.24	0.30 ± 0.01	0.55 ± 0.10	2.92 ± 1.08
HCC1937	TNBC	Basal	0.73 ± 0.25	0.84 ± 0.15	1.10 ± 0.01	1.02 ± 0.07	>10
BT-20	TNBC	Basal A	0.35 ± 0.38	0.06 ± 0.01	1.71 ± 0.21	0.37 ± 0.20	>10
BT-549	TNBC	Basal B	0.81 ± 0.17	2.19 ± 0.59	1.30 ± 0.01	0.06 ± 0.27	1.73 ± 0.71
MDA-MB-436	TNBC	Basal B	0.90 ± 0.28	5.23 ± 3.94	1.23 ± 1.01	0.66 ± 0.35	>10
MDA-MB-468	TNBC	Basal B	0.19 ± 0.07	1.57 ± 0.29	0.32 ± 0.04	0.35 ± 0.22	1.85 ± 0.51
Hs578T	TNBC	Basal B	>10	>10	>10	>10	>10
MDA-MB-231	TNBC	Basal B	>10	0.40 ± 0.05	>10	>10	>10
CAMA-1		Luminal	0.36 ± 0.02	0.84 ± 0.71	0.65 ± 0.13	0.60 ± 0.47	>10
Sk-Br-3		Luminal	>10	0.75 ± 0.22	0.47 ± 0.01	0.40 ± 0.38	>10
AU565		Luminal	>10	>10	>10	0.95 ± 0.15	>10
T47D		Luminal	>10	0.33 ± 0.18	>10	>10	>10
MDA-MB-453		Luminal A	0.82 ± 0.10	>10	>10	0.35 ± 0.06	>10
MCF-7		Luminal A	0.44 ± 0.21	0.35 ± 0.01	0.30 ± 0.09	>10	>10
BT-474		Luminal B	>10	0.47 ± 0.23	0.29 ± 0.04	0.05 ± 0.01	>10

IC_{50} values are averages of replicate independent assays, each determined by ten-point dosage treatments (n = 6 per dose).

and exhibited inhibition of only two kinases, FAK/PTK2 and JNK1, with IC_{50} values at 0.89 μM and 1.67 μM, respectively (see Supplemental Materials). Thus, compound **13** demonstrated selectivity for Mps1/TTK kinase.

2.4. Cell biology

To determine the functional cellular activity of candidate Mps1/TTK inhibitors, we monitored their effects on centriole assembly

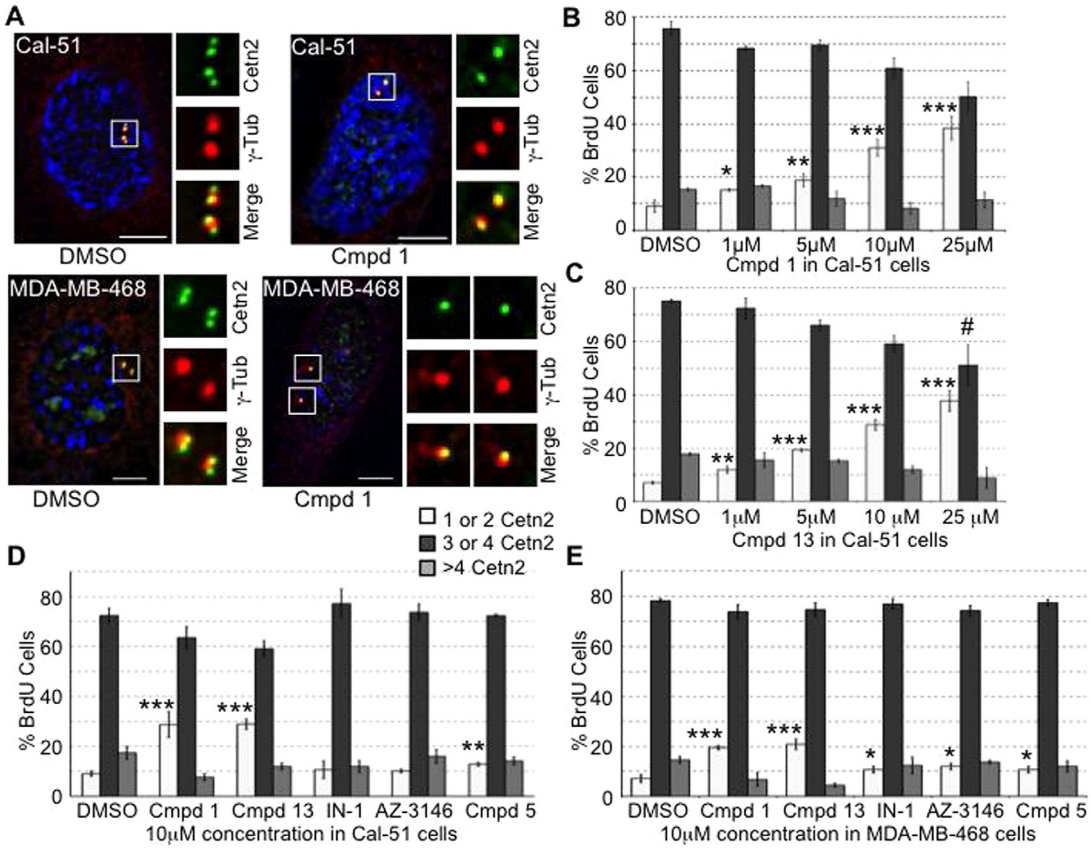

Fig. 3. Compound **1** and compound **13** attenuate centriole duplication in breast cancer cells. (A) Representative image of BrdU positive Cal-51 cells (top panel) and MDA-MB-468 cells (bottom panel) treated with either DMSO or compound **1** (25 μM). Cetn2 (green) was used as a centriolar marker and γ-tubulin (red) was used as a pericentriolar matrix (PCM) marker. Scale bar: 5 μM. Graphical representation of BrdU positive Cal-51 cells showing inhibition of centriole duplication with different concentrations of (B) compound **1** and (C) compound **13**. Compounds **1** and **13** led to an increase in the number of BrdU positive cells with 2 Cetn2 foci (off-white bar) in a concentration dependent manner. (D) Graphical representation of BrdU positive Cal-51 cells comparing the effect of different Mps1 inhibitors on centriole numbers. Compounds **1** and **13** increased the number of cells with 2 Cetn2 foci when compared to other inhibitors and DMSO control. DMSO and compound 5 were used as negative controls. (E) Graphical representation of BrdU positive MDA-MB-468 cells comparing the effect of different compounds on centriole numbers. Similar to that seen in Cal-51 cells, compounds **1** and **13** led to an increase in the number of cells with 2 Cetn2 foci. These experiments were done in triplicates and at least 75 cells were counted per replicate with the exception of 25 μM compound **13** in 4C (#); due to high amount of cell death in these samples, only 15 cells were counted in triplicate. Asterisks indicate P values calculated using two-sided Student's t-Test when comparing the percentage of cells with 1 or 2 centrioles for each indicated treatment to that for DMSO as follows: *, $P < 0.05 < P > 0.01$; **, $P < 0.01 < P > 0.005$; ***, $P < 0.005$.

and the spindle checkpoint. For centriole assembly assays (Fig. 3), Cal-51 and MDA-MB-468 cells were treated with candidate compounds prior to a short pulse of BrdU. Because the centriole pair is replicated at the G1/S transition, compounds that block centriole assembly will lead to an increased number of BrdU-positive cells with two centrioles. In addition, like many breast cancer cells Cal-51 and MDA-MB-468 are capable of centrosome amplification, and compounds that block this centrosome amplification should reduce the number of BrdU-positive cells with more than four centrioles. Roughly 80% of BrdU-positive DMSO-treated Cal-51 cells have three or four centrioles, but treatment with compound **1** or compound **13** leads to a dose dependent increase in the percentage of BrdU positive cells that have failed to complete centriole assembly and have just two centrioles (Fig. 3A–C). Compounds **1** and **13** also blocked centrosome amplification in Cal-51 cells, as evidenced by a dose dependent reduction in the percentage of cells with more than four centrioles. We also observed a decrease in cell viability at higher concentrations (10 μM and above) of compound **13** compared to the DMSO control and compound **1**. At 25 μM concentration of compound **13** there was a reduction in cell viability by 70% making it difficult to assay BrdU positive cells for centriole numbers (Fig. 3C). At 10 μM compounds **1** and **13** increased the percentage of BrdU positive Cal-51 cells with two centrioles compared to other Mps1 inhibitors (Fig. 3D). At 10 μM compounds **1** and **13** elicited similar effects in MDA-MB-468 cells (Fig. 3E) on centriole biogenesis during S-phase. On the other hand, the effects of AZ3146 and Mps1-IN-1 at the same concentrations on centriole assembly and centrosome amplification was similar to that of compound **5** that did not inhibit Mps1 kinase activity *in vitro* and was included as a negative control (Fig. 3D, E).

For SAC assays (Fig. 4), S-phase arrested cells treated with candidate compounds were released into medium containing the spindle poison nocodazole. Because the SAC prevents the metaphase to anaphase transition in the presence of spindle damage, cells with an intact SAC should arrest at metaphase with high levels of cyclin B in response to nocodazole. However, compounds that block the SAC will prevent this arrest, leading to a decreased number of mitotic cells and the loss of cyclin B. Roughly 40% of Cal-51 cells were arrested in mitosis after being released from S-phase arrest into nocodazole, but compound **1** leads to a dose-dependent reduction in the ability of cells to arrest in response to nocodazole (Fig. 4A, B). Compound **13** showed the maximal effect at 1 μM, the lowest concentration tested (Fig. 4B), and both compounds **1** and **13** are more effective than IN-1, AZ3146, or compound **5** that was included as a negative control (Fig. 4C). Compounds **1** and **13** had similar effects in MDA-MB-468 cells (Fig. 4C). In addition, compounds **1** and **13** lead to a loss of Cyclin B that required proteasome activity (Fig. 4D, E), and the loss was more pronounced than that observed in cells treated with either IN-1 or AZ3146 (Fig. 4F).

2.5. Solubility and pharmacokinetics of compound *13*

Solubility of compound **13** in DMSO was determined to be 53.4 mg/ml. Its solubility in the formulation of DMSO: Tween 80: PEG400: saline (10: 5: 10: 75) was 5 mg/ml. The formulation was then used for the pilot plasma pharmacokinetic studies in mice using intravascular (IV) and extravascular (IP) administrations (Supplemental Materials). Systemic clearance following an IV dose was 17.5 L/h/kg or roughly 3× mouse liver blood flow, suggesting considerable extrahepatic clearance. The elimination half-life was

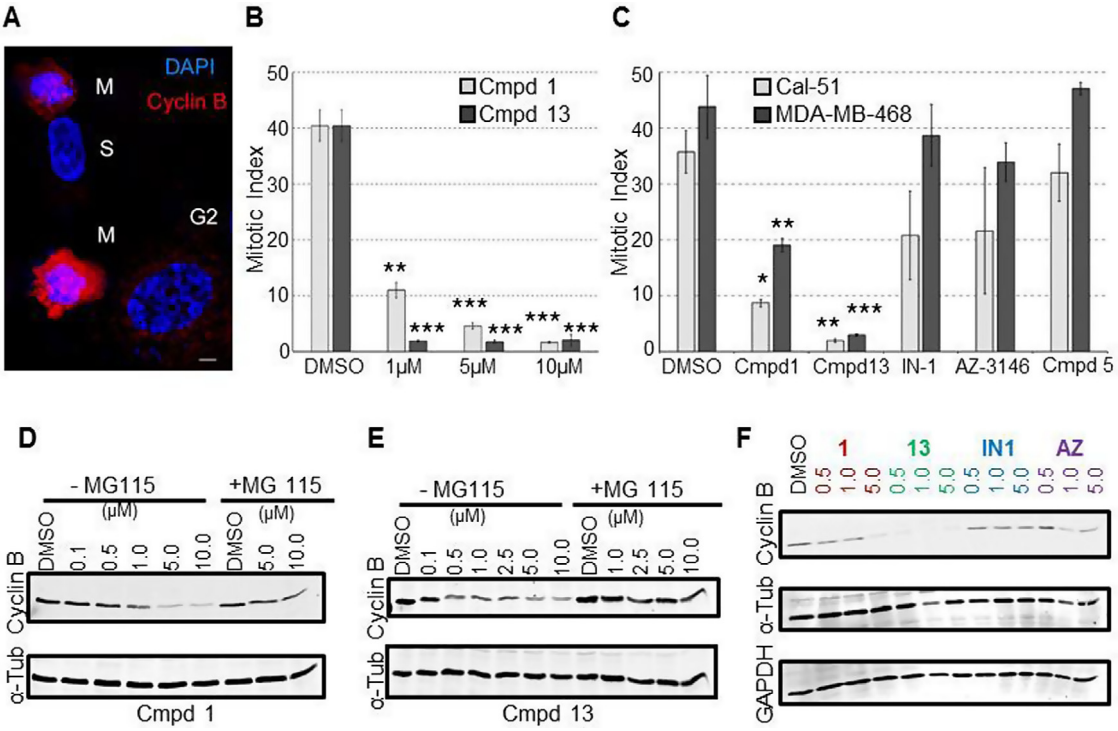

Fig. 4. Compound **1** and compound **13** attenuate the spindle assembly checkpoint in breast cancer cells. (A) Representative image of Cal-51 cells stained with DAPI (blue) and Cyclin B (red) showing a cell in S-phase (**S**), two cells in Mitosis (M) and a cell in G_2. (B) Graphical representation of the percentage of mitotic cells in the presence of different concentrations of compound **1** (light grey) and compound **13** (dark grey) compared to DMSO control in Cal-51 cells. (C) Graphical representation of the percentage of Cal-51 (light grey) or MDA-MB-468 cells (dark grey) cells in mitosis in the presence of various compounds. These experiments were done in triplicates and at least 500 cells were counted per set. (D-F) Cyclin B immunoblots from nocodazole treated Cal-51 cells in the presence of the indicated concentrations (in μM) of (D) compound **1** and (E) compound **13** with or without MG115, (F), and in the presence of increasing concentrations (in μM) of various compounds. Compound **13** has the strongest effect on Cyclin B levels. Asterisks indicate P values calculated using two-sided Student's *t*-Test when comparing the mitotic index for each indicated treatment to that for DMSO as follows: *, $P < 0.05 < P > 0.01$; **, $P < 0.01 < P > 0.005$; ***$P < 0.005$.

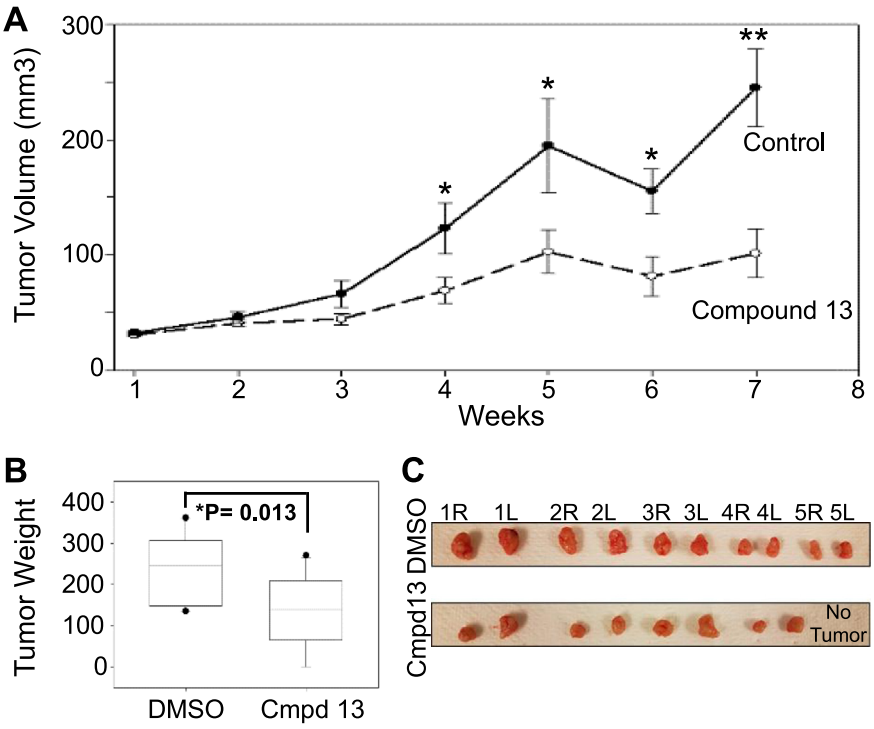

Fig. 5. Compound **13** reduces the growth of breast cancer cell derived xenografts in immunodeficient mice. Athymic nude mice carrying Cal-51 cells derived xenografts were treated after 1 week with either DMSO control or compound **13** inhibitor i.p., once daily and the tumor area was routinely measured using a caliper. (A) Graphical representation of tumor volume data (mean) of compound **13** injected mice (black dotted line) compared to control DMSO treated mice (black solid line) over a period of 7 weeks. The P values for the weeks are as follows; week 3 :0.08, week 4 :0.029, week 5 :0.042, week 6 :0.011, week 7 :0.002. Error bars indicate SEM and the P values were calculated using two-sided Student's *t*-test. $^{*}P < 0.05$, $^{**}P < 0.01$. (B) Box and whisker plot showing the weight of tumors dissected from mice sacrificed at week 7 after inoculation. The dots represent the outliers. (C) Representative image of tumors dissected from DMSO treated mice compared to tumors from compound **13** treated mice at week 7.

2.28 h. The IP AUC was determined to be 20,031 h ∗ nmol/L or 8463 h ∗ ng/mL following a 50 mg/kg dose. These data suggest that an IP administration of compound **13** at doses up to 50 mg/kg could reasonably be expected to provide a level of drug sufficient for the inhibition of Mps1 driven tumor growth.

2.6. In vivo evaluation in breast cancer xenograft model

To explore the effects of compound **13** on tumor growth *in vivo*, athymic nude mice were injected with the highly tumorigenic Cal 51 breast cancer cells. After the tumors reached a certain size, mice were injected every day with either compound **13** (10 mg/kg) or DMSO (control). The growth rates of the xenografts in compound **13** administered mice were significantly reduced compared to those in DMSO control mice (Fig. 5A–C). The reduction in growth rates was first observed after 3 weeks of initiation of drug administration (Fig. 5A). This reduced growth rate was observed until the mice were sacrificed at week 7, when the most significant reduction was observed ($p = 0.002$). There was also a significant reduction in the tumor weight of the compound **13** treated mice compared to the control mice (Fig. 5B). Overall, the data suggest that compound **13** significantly inhibited growth of xenografted tumors in nude mice and had no toxic effect on the mice, as there was no significant change in body weight over the course of the experiment (Supplemental Materials).

3. Discussion

Current therapies for aggressive types of breast cancer such as TNBC rely heavily on chemotherapy that can also affect non-cancer cells that divide quickly such as bone marrow cells, lining of the intestines and hair follicles. Hence, there is an urgent need for newer targeted therapies.

To facilitate the advancement of targeted therapies, studying the basic molecular mechanisms that underlie the progression of a cell from normalcy to tumor onset and metastasis is crucial. A high frequency of aneuploidy is commonly observed in cancer. While normal mammalian cells are highly intolerant to aneuploidy, cancer cells develop the capacity to tolerate and thrive with high frequency of aneuploidy. Expression of checkpoint genes are frequently increased in cancers when compared to normal cells.[43,44] Also, high levels of Mps1 are observed in breast cancer cells and reducing Mps1 levels in aneuploid cells increases the frequency of aberrant mitoses and decreases survival.[5] In addition, Mps1 inhibitor studies have shown SAC inactivation, which increased aneuploidy and aberrant mitoses resulting in cell death in cancer cells.[45,46] These data suggest that Mps1 is a good anticancer target.

Centrosome amplification is prevalent in breast cancer cells.[23] This represents a potential target unique to cancer cells, and a recent study reported that an inhibitor of the centrosome regulator Plk4 kinase had potent antitumor activity.[47] In our study, novel small molecules targeting Mps1 were designed by computer assisted docking analyses, and several candidate compounds were synthesized. These compounds were evaluated in anti-proliferative assays of a panel of 15 breast cancer cell lines and further examined for their ability to inhibit a variety of Mps1-dependent biological functions. The results indicate that the lead compounds have strong anti-proliferative potential through Mps1/TTK inhibition in both basal and luminal BC cell lines, exhibiting IC_{50} values

ranging from 0.05 to 1.0 μM. In addition, lead compounds **1** and **13** inhibit Mps1 kinase enzymatic activity with IC_{50} values 0.809 μM and 0.356 μM, respectively. In functional cellular assays, compounds **1** and **13** produced a dose-dependent increase in the percentage of BrdU positive cells that have failed to complete centriole assembly and also blocked centrosome amplification. Furthermore, both compounds **1** and **13** were the most effective at abrogating the spindle checkpoint.

Based on the computational study of the chemical scaffold (Fig. 1), the addition of fragments into Site 1 did enhance potency and selectivity, with both the cyclohexyl moiety (compound **13**) and the isopropylsulfonylphenyl moiety (compound **1**) resulting in excellent inhibition. In addition, the fragments at Site 2, a 4-morpholinophenyl (compound **13**) and a 4-hydroxypiperidinyl (compound **1**), led to increased activity and improved drug properties such as solubility.

Unlike other Mps1 inhibitors, compounds **1** and **13** prevent centrosome amplification. It will be interesting to determine in the future whether the primary efficacy of these compounds is through their effects on centrosomes, on the SAC, or on other Mps1 functions. Because tumors consist of a heterogeneous population of cells with and without centrosome amplification, it would also be interesting to test how depletion of a population of cells with centrosome amplification affects the overall tumor progression.

The most promising analog, compound **13**, was selected for *in vivo* evaluation. Compound **13** in the formulation of DMSO: Tween 80: PEG400: saline (10: 5: 10: 75) was used for the pilot plasma pharmacokinetic studies in mice. The extravascular (IP) administrations resulted in an AUC of 20,031 h ∗ nmol/L following a 50 mg/kg dose, suggesting excellent bioavailability. A dose of 10 mg/kg of compound **13** was selected for evaluation of antitumor activity in nude mice containing Cal 51 breast cancer cell xenografts. At this dose, compound **13** significantly decreased tumor growth over the 7-week study.

In summary, novel small molecule Mps1/TTK inhibitors have been identified as potential targeted therapies for basal and luminal types of breast cancers using drug discovery technologies, computational modeling, medicinal chemistry, cell culture and *in vivo* assays. Since Mps1 has many critical roles in cells, future in-depth investigations of both anticancer activities and safety profiles of these Mps1 inhibitors are warranted.

4. Materials and methods

Proton (^1H) and Carbon (^{13}C) NMR spectrums were obtained on Bruker 300 MHz FT-NMR and Bruker 400 MHz FT-NMR instrument at College of Pharmacy, The Ohio State University. High Resolution Mass Spectrums (HR-MS) were obtained on Micromass LCT spectrometer at the Campus Chemical Instrumentation Center of The Ohio State University. All chemicals and solvents were purchased from standard commercial suppliers.

4.1. Computational drug design

AutoDock version 4.0.0[48,49] was used for the docking simulation. The Lamarckian genetic algorithm (LGA) was selected for ligand conformational searching because it has enhanced performance relative to simulated annealing or the simple genetic algorithm. For all compounds, all hydrogens were added and Gasteiger charges[50] were assigned, then non-polar hydrogens were merged. 80 × 100 × 70 3-D affinity grids centered on the empty binding site with 0.375 Å spacing were calculated for each of the following atom types: a) protein: A (aromatic C), C, HD, N, NA, OA, SA; b) ligand: C, A, OA, HD, NA, SA, e (electrostatic) and d (desolvation) using Autogrid4. The ligand's translation, rotation and internal torsions are defined as its state variables and each gene represents a state variable. LGA adds local minimization to the genetic algorithm, enabling modification of the gene population. The docking parameters were as follows: trials of 100 dockings, population size of 250, random starting position and conformation, translation step ranges of 2.0 Å, rotation step ranges of 50°, elitism of 1, mutation rate of 0.02, crossover rate of 0.8, local search rate of 0.06, and 100 million energy evaluations. Final docked conformations were clustered using a tolerance of 1.5 Å root-mean-square deviations (RMSD).

4.2. Chemistry

4.2.1. tert-Butyl 2-chloro-4-((2-(isopropylsulfonyl)phenyl)amino)-7H-pyrrolo[2,3-d]pyrimidine-7-carboxylate (**4**)

The synthesis of *tert*-butyl 2,4-dichloro-7H-pyrrolo[2,3-*d*] pyrimidine-7-carboxylate (**3**) was achieved from compound **2** according to reported procedure.[41] For the synthesis of *tert*-butyl 2-chloro-4-((2-(isopropylsulfonyl)phenyl)amino)-7H-pyrrolo[2,3-*d*]pyrimidine-7-carboxylate **(4)**, *tert*-butyl 2,4-dichloro-7H-pyrrolo [2,3-*d*]pyrimidine-7-carboxylate (**3**, 0.239 g, 0.83 mmol), 2-(isopropylsulfonyl)-aniline (0.165 g, 0.83 mmol) and K_2CO_3 (0.220 g, 1.6 mmol) was dissolved in 3 mL *t*-butanol. The reaction mixture was degassed for 15 min. $Pd_2(dba)_3$ (0.046 g, 0.05 mmol) and XPhos (0.036 g, 0.076 mmol) was added to the reaction mixture under nitrogen atmosphere and stirred for 4 h at 100 °C. The reaction mixture was cooled to room temperature, filtered, and partitioned between ethyl acetate and water. The aqueous layer was extracted three times with ethyl acetate. The combined organic layer was washed with water and brine, dried over sodium sulfate and concentrated under reduced pressure. Product **4** was purified using silica gel column chromatography with 20–30% ethyl acetate – hexane mixture as the solvent system (solid; yield 56%). ^1H NMR (300 MHz, $CDCl_3$) δ 9.97 (s, 1H), 8.82 (d, J = 8.5 Hz, 1H), 7.87 (d, J = 7.7 Hz, 1H), 7.72 (t, J = 7.3 Hz, 1H), 7.53 (d, J = 4.0 Hz, 1H), 7.25 (t, J = 7.7 Hz, 1H), 6.59 (d, J = 3.9 Hz, 1H), 3.23 (m, 1H), 1.68 (s, 9H), 1.30 (d, J = 6.8 Hz, 6H).

4.2.2. tert-Butyl 2-((4-(4-hydroxypiperidin-1-yl)-2-methoxyphenyl) amino)-4-((2-(isopropylsulfonyl)phenyl)amino)-7H-pyrrolo[2,3-d] pyrimidine-7-carboxylate (**5**)

tert-Butyl 2-chloro-4-((2-(isopropylsulfonyl)phenyl)amino)-7H-pyrrolo[2,3-*d*]pyrimidine-7-carboxylate (**4**, 0.211 g, 0.47 mmol), 1-(4-amino-3-methoxyphenyl)piperidin-4-ol (0.125 g, 0.56 mmol) and K_2CO_3 (0.195 g, 1.41 mmol) was dissolved in 2 mL *t*-butanol. The reaction mixture was degassed for 15 min. $Pd_2(dba)_3$ (0.025 g, 0.028 mmol) and XPhos (0.020 g, 0.042 mmol) was added to the reaction mixture under nitrogen atmosphere and stirred for 6 h at 100 °C. The reaction mixture was processed in the same manner as Compound **4**. Product **5** was purified using silica gel column chromatography with 80–90% ethyl acetate – hexane mixture as the solvent system (solid, yield 59%). ^1H NMR (300 MHz, $CDCl_3$) δ 8.37 (d, J = 5.1 Hz, 1H), 7.99 (d, J = 5.2 Hz, 1H), 7.89 (s, 1H), 7.55 (m, 2H), 7.38–7.25 (m, 1H), 7.24–7.03 (m, 1H), 6.84 (s, 1H), 6.59 (s, 1H), 6.53 (d, J = 4.2 Hz, 1H), 6.30 (d, J = 4.0 Hz, 1H), 4.24–4.05 (m, 1H), 3.87 (m, 4H), 3.50 (m, 2H), 3.29 (m, 1H), 2.91 (m, 2H), 2.06 (m, 2H), 1.78 (m, 2H), 1.69 (s, 9H), 1.29 (d, J = 3.6 Hz, 6H).

4.2.3. 1-(4-((4-((2-(Isopropylsulfonyl)phenyl)amino)-7H-pyrrolo[2,3-d]pyrimidin-2-yl)amino)-3-methoxyphenyl)piperidin-4-ol (Compound **1**)

tert-Butyl 2-((4-(4-hydroxypiperidin-1-yl)-2-methoxyphenyl) amino)-4-((2-(isopropylsulfonyl)phenyl)amino)-7H-pyrrolo[2,3-*d*] pyrimidine-7-carboxylate (**5**, 0.063 g, 0.10 mmol) was dissolved in 5 mL DCM. 1 mL TFA was added to the reaction mixture and stirred

for 4 h at room temperature. The reaction was neutralized with saturated $NaHCO_3$ solution and extracted three times with ethyl acetate. The combined organic layer was washed with water and brine, dried over sodium sulfate and was concentrated under reduced pressure. **Compound 1** was purified using preparative thin layer chromatography with ethyl acetate and few drops of methanol as the solvent system (solid, yield 35%). ^{1}H NMR (300 MHz, DMSO-d_6) δ 11.40 (s, 1H), 9.48 (s, 1H), 8.81 (d, J = 8.4 Hz, 1H), 7.81 (m, 2H), 7.74–7.66 (m, 1H), 7.50 (s, 1H), 7.36–7.17 (m, 1H), 6.99 (s, 1H), 6.64 (s, 1H), 6.48 (d, J = 9.9 Hz, 1H), 6.22 (s, 1H), 4.69 (d, J = 3.2 Hz, 1H), 3.81 (s, 3H), 3.72–3.55 (m, 1H), 3.58–3.39 (m, 3H), 2.80 (t, J = 11.2 Hz, 2H), 1.93–1.77 (m, 2H), 1.65–1.41 (m, 2H), 1.17 (d, J = 6.2 Hz, 6H). HR-MS (M +Na)$^+$ calculated 559.2103; observed 559.2132.

4.2.4. tert-Butyl 4-((2-(isopropylsulfonyl)phenyl)amino)-2-((2-methoxy-phenyl)amino)-7H-pyrrolo[2,3-d]pyrimidine-7-carboxylate (**6**)

tert-Butyl 2-chloro-4-((2-(isopropylsulfonyl)phenyl)amino)-7H-pyrrolo[2,3-*d*]pyrimidine-7-carboxylate (**4**, 0.350 g, 0.78 mmol), 2-methoxyaniline (0.106 g, 0.86 mmol) and K_2CO_3 (0.317 g, 2.3 mmol) was dissolved in 4 mL *t*-butanol. The reaction mixture was degassed for 15 min. $Pd_2(dba)_3$ (0.045 g, 0.049 mmol) and Xphos (0.040 g, 0.084 mmol) was added to the reaction mixture under nitrogen atmosphere and stirred for 6 h at 100 °C. The reaction mixture was processed in the same manner as Compound **4**. Product **6** was purified using silica gel column chromatography (solid, yield 49%). ^{1}H NMR (300 MHz, DMSO-d_6) δ 9.56 (s, 1H), 8.47 (d, J = 8.8 Hz, 1H), 8.40 (d, J = 7.2 Hz, 1H), 7.88 (d, J = 8.6 Hz, 1H), 7.78 (m, 2H), 7.42 (m, 2H), 7.02 (d, J = 7.8 Hz, 1H), 6.96 (t, J = 6.5 Hz, 1H), 6.84 (t, J = 8.1 Hz, 1H), 6.54 (d, J = 3.8 Hz, 1H), 3.87 (s, 3H), 3.50–3.33 (m, 1H), 1.63 (s, 9H), 1.13 (d, J = 6.8 Hz, 6H).

4.2.5. N4-(2-(isopropylsulfonyl)phenyl)-N2-(2-methoxyphenyl)-7H-pyrrolo-[2,3-d]pyrimidine-2,4-diamine (**7**)

tert-Butyl 4-((2-(isopropylsulfonyl)phenyl)amino)-2-((2-methoxyphenyl)amino)-7H-pyrrolo[2,3-*d*]pyrimidine-7-carboxylate (**6**, 0.100 g, 0.19 mmol) was deprotected in a manner similar as Compound **5**. **Compound 7** was purified using silica gel column chromatography (solid, yield 48%). ^{1}H NMR (300 MHz, DMSO-d_6) δ 11.51 (s, 1H), 9.48 (s, 1H), 8.71 (d, J = 8.5 Hz, 1H), 8.29 (d, J = 6.6 Hz, 1H), 7.84 (d, J = 7.9 Hz, 1H), 7.75 (t, J = 6.7 Hz, 1H), 7.63 (s, 1H), 7.32 (t, J = 6.8 Hz, 1H), 7.13–7.00 (m, 2H), 6.98–6.78 (m, 2H), 6.27 (s, 1H), 3.86 (s, 3H), 3.52–3.27 (m, 1H), 1.16 (d, J = 6.9 Hz, 6H). ^{13}C NMR (DMSO-d_6, 75 MHz) δ 155.24, 152.69, 152.65, 148.31, 139.49, 135.06, 130.85, 129.58, 123.47, 123.34, 122.54, 121.35, 121.01, 120.22, 119.35, 110.47, 98.88, 97.15, 55.65, 55.04, 14.80. HR-MS (M+Na)$^+$ calculated 460.1419; observed 460.1312.

4.2.6. tert-Butyl 4-((2-(isopropylsulfonyl)phenyl)amino)-2-((2-methoxy-4-morpholinophenyl) amino)-7H-pyrrolo[2,3-d]pyrimidine-7-carboxylate (**8**)

tert-Butyl 2-chloro-4-((2-(isopropylsulfonyl)phenyl)amino)-7H-pyrrolo[2,3-*d*]pyrimidine-7-carboxylate (**4**, 0.350 g, 0.78 mmol), 2-methoxy-4-morpholinoaniline (0.162 g, 0.78 mmol) and K_2CO_3 (0.317 g, 2.3 mmol), was dissolved in 4 mL *t*-butanol. The reaction mixture was degassed for 15 min. $Pd_2(dba)_3$ (0.045 g, 0.049 mmol) and Xphos (0.040 g, 0.084 mmol) was added to the reaction mixture under nitrogen atmosphere and stirred for 4 h at 100 °C. The reaction mixture was processed in the same manner as Compound **4**. Product **8** was purified using silica gel column chromatography (solid, yield 42%). ^{1}H NMR (300 MHz, $CDCl_3$) δ 9.58 (s, 1H), 8.85 (d, J = 8.4 Hz, 1H), 8.49 (d, J = 9.1 Hz, 1H), 7.91 (d, J = 7.4 Hz, 1H), 7.67 (t, J = 8.0 Hz, 1H), 7.55 (s, 1H), 7.33 (d, J = 4.0 Hz, 1H), 7.23 (t, J = 7.8 Hz, 1H), 6.58 (d, J = 10.2 Hz, 2H), 6.51 (d, J = 4.0 Hz, 1H), 3.91 (m, 7H), 3.37–3.22 (m, 1H), 3.21–3.13 (m, 4H), 1.74 (s, 9H), 1.34 (d, J = 6.8 Hz, 6H).

4.2.7. N4-(2-(Isopropylsulfonyl)phenyl)-N2-(2-methoxy-4-morpholinophenyl)-7H-pyrrolo[2,3-d]pyrimidine-2,4-diamine (**9**)

tert-Butyl 2-chloro-4-((2-(isopropylsulfonyl)phenyl)amino)-7H-pyrrolo[2,3-*d*]pyrimidine-7-carboxylate (**8**, 0.100 g, 0.16 mmol) was deprotected in a manner similar as Compound **5**. **Compound 9** was purified using silica gel column chromatography (solid, yield 36%). ^{1}H NMR (300 MHz, $CDCl_3$) δ 9.52 (s, 1H), 9.28 (s, 1H), 8.88 (d, J = 8.2 Hz, 1H), 8.27 (d, J = 8.6 Hz, 1H), 7.89 (dd, J = 8.1, 1.3 Hz, 1H), 7.65 (t, J = 7.2 Hz, 1H), 7.19 (dd, J = 9.1, 5.8 Hz, 2H), 6.80–6.73 (m, 1H), 6.60 (d, J = 2.4 Hz, 1H), 6.55 (dd, J = 9.0, 1.7 Hz, 1H), 6.47–6.37 (m, 1H), 3.90 (m, 7H), 3.29 (dt, J = 13.9, 6.9 Hz, 1H), 3.21–3.10 (m, 4H), 1.32 (d, J = 6.9 Hz, 6H). HR-MS (M+Na)$^+$ calculated 545.1947; observed 545.1882.

4.2.8. 2-Chloro-N-cyclohexyl-7H-pyrrolo[2,3-d]pyrimidin-4-amine (**10**)

2,4-Dichloro-7H-pyrrolo[2,3-*d*]pyrimidine **2** (0.695 g, 3.75 mmol), cyclohexyl amine (0.406 g, 4.1 mmol) and TEA (0.758 g, 7.5 mmol) were dissolved in 18 mL ethanol and refluxed overnight. The solvent was reduced and the residue was dissolved in ethyl acetate. The organic layer was washed with water and brine, dried over sodium sulfate and concentrated under reduced pressure. Compound **10** was purified by silica gel column chromatography with 30–40% EA-Hex mixture (solid, yield 78%). ^{1}H NMR (300 MHz, DMSO-d_6) δ 11.60 (s, 1H), 7.60 (d, J = 7.6 Hz, 1H), 7.40 (d, J = 3.8 Hz, 1H), 6.60 (d, J = 3.3 Hz, 1H), 3.95 (m, 1H), 1.94–1.90 (m, 2H), 1.77–1.74 (m, 2H), 1.65–1.61 (m, 1H), 1.42 –1.20 (m, 4H), 1.18–1.13 (m, 1H).

4.2.9. tert-Butyl 2-chloro-4-(cyclohexylamino)-7H-pyrrolo[2,3-d] pyrimidine-7-carboxylate (**11**)

2-Chloro-N-cyclohexyl-7H-pyrrolo[2,3-*d*]pyrimidin-4-amine (**10**, 0.400 g, 1.6 mmol) was dissolved in 6 mL of DCM . Di-*tert*-butyl dicarbonate (0.419 g, 1.92 mmol), DIEA (0.248 g, 1.92 mmol) and DMAP (0.010 g, 0.08 mmol) was added to the reaction mixture and refluxed for 10 min. The reaction mixture was cooled, diluted with water and the aqueous layer was extracted three times with DCM. The combined organic layer was washed with water and brine, dried over sodium sulfate and concentrated under reduced pressure. Product **11** was purified using silica gel column chromatography with 5–10% ethyl acetate – hexane mixture as the solvent system (solid, yield 85%). ^{1}H NMR (300 MHz, DMSO-d_6) δ 7.90 (d, J = 7.6 Hz, 1H), 7.40 (d, J = 3.8 Hz, 1H), 6.86 (d, J = 3.3 Hz, 1H), 3.94 (m, 1H), 1.93 (m, 2H), 1.73 (m, 2H), 1.57 (s, 9H), 1.32 (m, 4H), 1.17 (m, 2H).

4.2.10. tert-Butyl 4-(cyclohexylamino)-2-((2-methoxy-4-morpholinophenyl)amino)-7H-pyrrolo[2,3-d]pyrimidine-7-carboxylate (**12**)

tert-Butyl 2-chloro-4-(cyclohexylamino)-7H-pyrrolo[2,3-*d*] pyrimidine-7-carboxylate (**11**, 0.518 g, 1.48 mmol), 2-methoxy-4-morpholinoaniline(0.323 g, 1.55 mmol) and K_2CO_3 (0.290 g, 2.1 mmol) was dissolved in 4 mL *t*-butanol. The reaction mixture was degassed for 15 min. $Pd_2(dba)_3$ (0.068 g, 0.075 mmol) and XPhos (0.048 g, 0.102 mmol) was added to the reaction mixture under nitrogen atmosphere and stirred for 6 h at 100 °C. The reaction mixture was processed in the same manner as Compound **4**. Product **12** was purified using silica gel column chromatography with 60–70% ethyl acetate – hexane mixture as the solvent system (solid, yield 45%). ^{1}H NMR (300 MHz, DMSO-d_6) δ 8.48 (d, J = 8.8 Hz, 1H), 7.27 (d, J = 7.4 Hz, 1H), 7.17 (s, 1H), 7.14 (d, J = 4.0 Hz, 1H), 6.71 (d, J = 4.0 Hz, 1H), 6.66 (d, J = 2.3 Hz, 1H), 6.43 (dd, J = 8.9, 2.1 Hz, 1H), 3.98 (m, 1H), 3.89 (s, 3H), 3.81–3.70

(m, 4H), 3.15–3.01 (m, 4H), 1.96 (m, 1H), 1.78 (d, J = 9.8 Hz, 2H), 1.73–1.67 (m, 1H), 1.60 (s, 9H), 1.44–1.21 (m, 6H).

4.2.11. N4-Cyclohexyl-N2-(2-methoxy-4-morpholinophenyl)-7H-pyrrolo[2,3-d]pyrimidine-2,4-diamine (**13**)

tert-Butyl 4-(cyclohexylamino)-2-((2-methoxy-4-morpholinophenyl)amino)-7H-pyrrolo[2,3-*d*]pyrimidine-7-carboxylate (**12**, 0.100 g, 0.19 mmol) was deprotected in a manner similar as Compound **5**. The product, **Compound 13**, was purified using silica gel column chromatography with 90% ethyl acetate-hexane as the solvent system (solid, yield 33%). ^{1}H NMR (300 MHz, DMSO-d_6) δ 11.22 (s, 1H), 8.10 (s, 1H), 7.72 (s, 2H), 6.83 (s, 1H), 6.67 (d, J = 2.1 Hz, 1H), 6.55 (s, 1H), 6.49 (dd, J = 8.8, 2.1 Hz, 1H), 3.96 (d, J = 5.6 Hz, 1H), 3.86 (s, 3H), 3.80–3.69 (m, 4H), 3.16–3.02 (m, 4H), 1.97–1.80 (d, J = 10.2 Hz, 2H), 1.78 (d, J = 10.2 Hz, 2H), 1.67 (m, 1H), 1.35–1.25 (m, 5H). ^{13}C NMR (DMSO-d_6, 75 MHz) δ 171.96, 155.27, 154.55, 149.81, 148.83, 146.37, 122.48, 119.61, 118.01, 106.77, 99.94, 99.59, 96.90, 66.20, 55.64, 49.54, 49.10, 32.70, 25.39, 25.03, 21.00. HR-MS $(M+Na)^+$ calculated 445.2328; observed 445.2277.

4.3. Breast cancer cell culture

The human breast cancer cell lines MCF-7, MDA-MB-231, MDA-MB-453, MDA-MB-468, BT-20, Sk-Br-3, AU565, T47D CAMA-1 and BT-474 were purchased from American Type Culture Collection (ATCC, VA). Cal-51, HCC-1937, BT-549 cell lines were gift from Dr. Ching-Shih Chen (The Ohio State University). Hs578T and MDA-MB-436 cell lines were provided by Dr. Majumder Sarmila (The Ohio State University). The cells, except Sk-Br-3, AU565 and BT-474, were maintained in a mixture of Dulbecco's modified Eagle's medium and Ham's F12 medium (1:1) (DMEM/F12) without phenol red (Sigma-Aldrich, MO) supplemented with 5% fetal bovine serum (FBS, Sigma-Aldrich, MO) and 1x antibiotic–antimycotic (100 U/mL penicillin G sodium, 100 μg/mL streptomycin sulfate and 0.25 μg/mL amphotericin B, Life Technologies) and were plated separately in flasks in a humidified incubator (5% CO_2: 95% air, 37 °C). The media used for Sk-Br-3, AU565 and BT-474 cell lines was described previously.[51,52] The media were changed every 2–3 days. When the cells grew to about 80% confluence, cells were washed twice with calcium- and magnesium-free phosphate-buffered saline (PBS, pH 7.4), and then trypsinized with 0.05% trypsin–5.3 mm EDTA (Life Technologies). The trypsinization was stopped by addition of culture medium with 5% FBS. After centrifugation, the dissociated cells were resuspended in the same medium and subcultured into 75-cm^2 culture flasks at a ratio of 1:5 flasks.

4.4. Cell proliferation assays

All cells used for this assay were cultured in the DMEM/F-12 culture medium without Phenol Red supplemented with dextran-coated charcoal (DCC) (Dextran T-70, activated charcoal)-stripped 5% FBS for 24 h prior to seeding in a 96-well plate. A total of 1000 cells/100 μL/well were seeded and cultured in sextuple wells in DMEM/F12 supplemented with DCC treated FBS (5%) for another 24 h. The cells were then treated with presence or absence of candidate compound in fresh medium for treatments for 5–7 days. Antiproliferation effect of the potential compounds were assessed using CellTiter 96® AQueous solution (Promega, WI) assay according to the manufacturer's instructions. The plates were incubated for designated time duration and the color density was measured as the optical density at 490 nm using a microplate reader (Molecular Devices, CA). The IC_{50} value was determined as the concentration of compound required to reduce cell viability by 50% of the DMSO control group. GraphPad Prism 5 was used to calculate the IC_{50} values.

4.5. Mps1/TTK kinase activity assay

The inhibition potency to Mps1 kinase activity was determined by measurement of radioactive phosphotransfer to the specific substrate, Cetn2. The autophosphorylation of Mps1 was also measured using the same method without adding Cetn2 in the kinase assay reaction mixture. The absolute Km values for ATP and the Cetn2 were initially determined and each reaction was carried out at optimum ATP and Cetn2 concentrations, 2xKm and 5xKm, respectively. Mps1 activity was measured using 0.25 ng of recombinant GST-Mps1 protein[12] in 50 mM TrisCl pH 7.5, 0.5 mM DTT, 10 mM $MgCl_2$, 300 μM recombinant Cetn2 and 3 μM ^{32}P-γ-ATP. The assay was run in a 96 well plate; eleven serial 1:4 compound dilutions (from 0.025 nM to 25 μM) were tested to determine IC_{50} values. ATP was added to initiate the kinase assay, incubated at 30 °C for 30 min and fivefold volume of 50 μM EDTA was added to quench the reaction. The whole reaction was immobilized on Immobilon-P^{SQ} PVDF membrane (Millipore) using a dot blotter (BioRad) connected to vacuum line. Each well was washed three times with 300 μL of PBS. The membrane was further washed by soaking in PBS, dried, and exposed overnight to a Phosphor Screen. The image was acquired by the Storm imaging system (Amersham). The density analyses were performed by using Image-J program, and IC_{50} values were calculated by GraphPad Prism 5 software. Commercial kinase profiling assays were performed by Reaction Biology Corp., Malvern, PA.

4.6. Cell biology assays

Cells were plated onto fibronectin (Sigma-Aldrich) coated coverslips in 24 well dishes using the medium and growth conditions described above, but using medium containing phenol red. At 24 h after plating, compounds (or the equivalent amount of DMSO) were added to individual wells at various concentrations. Cells were incubated for 24 h at 37 °C. 40 μM BrdU (Sigma-Aldrich) was added during the last 4 h of the incubation, after which cells were fixed in pre-chilled methanol at −20 °C for 10 min, stained with centrosome markers, then treated with acid to denature chromosomal DNA prior to staining for BrdU using rat anti-BrdU antibody (Abcam) as previously described.[53,54] To assess centriole biogenesis, centriole number was determined for triplicate samples in cells that had entered S-phase as judged by incorporation of BrdU. Primary antibodies used were mouse anti-γTubulin (pericentriolar material) (Sigma-Aldrich) and rabbit anti-Centrin 2 (centrioles).[24] Secondary antibodies used were Alexa350-conjugated goat anti-rat, Alexa594-conjugated donkey anti-mouse, and Alexa488-conjugated donkey anti-rabbit (Invitrogen).

To assess the integrity of the spindle assembly checkpoint, the ability of cells to arrest in mitosis in response to the spindle poison nocodazole was monitored.[54] Cells were synchronized in S-phase with a 24 h treatment with 2 mM thymidine (Sigma-Aldrich). Three hours after removing thymidine to release cells from S-phase arrest, nocodazole (Sigma-Aldrich) was added at 200 ng/mL. After 12 h in the presence of nocodazole, cells were fixed and stained with mouse anti-cyclin B (Cell Signaling Technology) and Hoechst (Sigma-Aldrich), and the percentage of cyclin B positive cells with condensed chromosomes was determined in triplicate samples.

4.7. Immunoblotting

Cal-51 cells were synchronized in mitosis using thymidine and nocodazole as described above. The proteasome inhibitor MG115 (Sigma-Aldrich) or DMSO was added 4 h prior to harvesting cells. Cells were lysed and run on a SDS-PAGE gel followed by immunoblotting. Primary antibodies used were rabbit anti-cyclin B (Cell Signaling Technology), mouse anti-α-tubulin (DM1A,

Sigma-Aldrich) and rabbit anti-GAPDH (Cell Signaling Technology). Secondary antibodies used were Alexa-680-conjugated donkey anti-mouse/rabbit (Invitrogen) and IRDye-800-conjugated donkey anti-mouse/rabbit (Rockland).

4.8. Drug solubility and pharmacokinetic analysis

The maximum solubility of compound **13** in DMSO and a formulation of DMSO: Tween 80: PEG400: saline (10: 5: 10: 75) was determined. The soluble fraction (saturated) was serially diluted and 100 μL of each sample were analyzed by absorption spectrometry using BioTek Synergy HT Multi-Mode Microplate Reader. The dilution of the original formulation solution falling within the linear range of the calibration curve was used to assess the concentration of test compound in the soluble fraction. Data were acquired by using Software Gen5 2.05.

For plasma pharmacokinetic analysis, a sterile dosing solution of compound **13** was prepared in DMSO: Tween 80: PEG400: saline (10: 5:10:75). Male ICR mice 6 weeks of age (Harlan Laboratories, Madison, WI) were dosed via IV (20 mpk) or IP (50 mpk) injection. The injection volumes were 100 μl for IV and 250 μl for IP per mouse (~25 g). Ten mice per compound for each dosing route were used to perform pilot PK study. At each of time points of 5, 10, 20, 30 min, and 1, 2, 4, 6, 8 and 24 h post dosing, one mouse was sacrificed by CO_2 asphyxiation, and blood was immediately collected via cardiac puncture then transferred to heparinized tubes. After centrifugation, plasma was separated and collected for storage at −80 °C until processing and analysis. The analysis was performed on a LC-MS/MS system consisting of Thermo Accela UHPLC pump, Thermo PAL autosampler and Thermo TSQ Discovery triple quadruple mass spectrometer. Mouse plasma samples were processed with a simple protein precipitation using acetonitrile, followed by chromatographic separation using an Agilent Zorbax Extend C18 column. An 8.0 min linear gradient elution was used at a flow rate of 400 μL/min with a mobile phase of water and acetonitrile, both modified with 0.1% formic acid. The analytes and internal standard, hesperetin, were detected by selected-reaction monitoring mode with positive electrospray ionization. Plasma concentration-time data was analyzed by non-compartmental methods using default settings and the NCA analysis object in Phoenix WinNonlin v6.3.

4.9. In vivo mouse xenograft study

The *in vivo* evaluation of compound **13** on tumor growth was examined in athymic nude mice injected with the highly tumorigenic Cal 51 breast cancer cells. Compound **13** stock solution (10 mg/mL) (or the equivalent amount of DMSO as control) was mixed with 5% Tween 80, 10% PEG 400, and then diluted with warm sterile 0.9% saline to achieve a final concentration of 1 mg/mL. The drug mixture and DMSO control were stored at 37 °C until use.

Cal 51 cells were grown in culture for one week prior to injections. Cells were spun down and resuspended in PBS and then mixed with equal volume of Matrigel (Corning). Approximately 1×10^6 cells/site were injected into the mammary fat pads, at two sites (left and right side in between the 4th and 5th mammary fat pads) of each athymic nude female mouse (TVSR core, OSU). The mice were randomized to control (DMSO) and drug (Compound **13**) groups. Drug administration was started when the tumors reached a size of approximately 0.4–0.55 cm in length. Compound **13** at 10 mg/kg or DMSO (control) was injected intraperitoneally (*i.p.*) in the lower right quadrant of the mice every 24 h. Tumors were measured weekly by using calipers and the tumor volume was estimated. Mice were euthanized 7 weeks post inoculation and tumor weight determined.

4.10. Statistical analysis

The statistical analysis was done using Student's *t* test (two tailed). Criterion for statistical significance was $p < 0.05$. ANOVA was used to analyze the overall drug impact in the xenograft mice study. For comparison at different time-points between the groups, Student's t-Tests were conducted using Statistics Software R3.2.0. All the tests were two-sided and the criterion for statistical significance was $P < 0.05$.

Conflict of interests

None.

Acknowledgements

This research was supported by the Pelotonia Fund and the Stephanie Spielman Fund for Breast Cancer Research, The Ohio State University Comprehensive Cancer Center. The research also received support from the OSU Center for Clinical and Translational Sciences through Grant UL1 TR001070 from the National Center For Advancing Translational Sciences, and Research Scholar Grant 10-248-01-TBG from the American Cancer Society to HAF. Solubility and pharmacokinetic evaluations were performed by the Pharmacoanalytical Shared Resource of the OSU Comprehensive Cancer Center, Grant P30 CA016058 from the National Cancer Institute, directed by Dr. Mitch Phelps and Dr. Christopher Coss. Dr. Junan Li, College of Pharmacy, provided statistical analysis for the *in vivo* study.

A. Supplementary material

Supplementary data associated with this article can be found, in the online version, at http://dx.doi.org/10.1016/j.bmc.2017.02.030.

References

1. Sorlie T, Perou CM, Tibshirani R, et al. Gene expression patterns of breast carcinomas distinguish tumor subclasses with clinical implications. *P Natl Acad Sci USA*. 2001;98:10869–10874.
2. Khalifeh IM, Albarracin C, Diaz LK, et al. Clinical, histopathologic, and immunohistochemical features of microglandular adenosis and transition into in situ and invasive carcinoma. *Am J Surg Pathol*. 2008;32:544–552.
3. Blows FM, Driver KE, Schmidt MK, et al. Subtyping of breast cancer by immunohistochemistry to investigate a relationship between subtype and short and long Term survival: a collaborative analysis of data for 10,159 cases from 12 studies. *Plos Medicine*. 2010;7:e1000279.
4. Brough R, Frankum JR, Sims D, et al. Functional viability profiles of breast cancer. *Cancer Discov*. 2011;1:260–273.
5. Daniel J, Coulter J, Woo JH, Wilsbach K, Gabrielson E. High levels of the Mps1 checkpoint protein are protective of aneuploidy in breast cancer cells. *P Natl Acad Sci USA*. 2011;108:5384–5389.
6. Maire V, Baldeyron C, Richardson M, et al. TTK/hMPS1 is an attractive therapeutic target for triple-negative breast cancer. *PLoS ONE*. 2013;8:e63712.
7. Winey M, Goetsch L, Baum P, Byers B. *MPS1* and *MPS2*: novel yeast genes defining distinct steps of spindle pole body duplication. *J Cell Biol*. 1991;114:745–754.
8. Lindberg RA, Fischer WH, Hunter T. Characterization of a human protein threonine kinase isolated by screening an expression library with antibodies to phosphotyrosine. *Oncogene*. 1993;8:351–359.
9. Mills GB, Schmandt R, McGill M, et al. Expression of TTK, a novel human protein kinase, is associated with cell proliferation. *J Biol Chem*. 1992;267:16000–16006.
10. Mills GB, Schmandt R, Mcgill M, et al. Expression of Ttk, a novel human protein-kinase, is associated with cell-proliferation. *J Biol Chem*. 1992;267:16000–16006.
11. Schmandt R, Hill M, Amendola A, Mills GB, Hogg D. Il-2-induced expression of Ttk, a serine, threonine, tyrosine kinase, correlates with cell-cycle progression. *J Immunol*. 1994;152:96–105.
12. Fisk HA, Mattison CP, Winey M. Human Mps1 protein kinase is required for centrosome duplication and normal mitotic progression. *P Natl Acad Sci USA*. 2003;100:14875–14880.
13. Kasbek C, Yang CH, Yusof AM, Chapman HM, Winey M, Fisk HA. Preventing the degradation of mps1 at centrosomes is sufficient to cause centrosome reduplication in human cells. *Mol Biol Cell*. 2007;18:4457–4469.

14. Kasbek C, Yang C-H, Fisk HA. Mps1 as a link between centrosomes and genetic instability. *Environ Mol Mutagen*. 2009;50:654–665.
15. Wei JH, Chou YF, Ou YH, et al. TTK/hMps1 participates in the regulation of DNA damage checkpoint response by phosphorylating CHK2 on threonine 68. *J Biol Chem*. 2005;280:7748–7757.
16. Saal LH, Gruvberger-Saal SK, Persson C, et al. Recurrent gross mutations of the PTEN tumor suppressor gene in breast cancers with deficient DSB repair. *Nature Genetics*. 2008;40:102–107.
17. Lingle WL, Barrett SL, Negron VC, et al. Centrosome amplification drives chromosomal instability in breast tumor development. *P Natl Acad Sci USA*. 2002;99:1978–1983.
18. Lingle WL, Salisbury JL. Altered centrosome structure is associated with abnormal mitoses in human breast tumors. *Am J Pathol*. 1999;155:1941–1951.
19. Lingle WL, Lutz WH, Ingle JN, Maihle NJ, Salisbury JL. Centrosome hypertrophy in human breast tumors: implications for genomic stability and cell polarity. *P Natl Acad Sci USA*. 1998;95:2950–2955.
20. Kasbek C, Yang CH, Fisk HA. Antizyme restrains centrosome amplification by regulating the accumulation of Mps1 at centrosomes. *Mol Biol Cell*. 2010;21:3879–3889.
21. Liu J, Cheng X, Zhang Y, et al. Phosphorylation of Mps1 by BRAFV600E prevents Mps1 degradation and contributes to chromosome instability in melanoma. *Oncogene*. 2013;32:713–723.
22. Salisbury JL, Whitehead CM, Lingle WL, Barrett SL. Centrosomes and cancer. *Biol Cell*. 1999;91:451–460.
23. Chan JY. A clinical overview of centrosome amplification in human cancers. *Int J Bio Sci*. 2011;7:1122–1144.
24. Yang CH, Kasbek C, Majumder S, Mohd Yusof A, Fisk HA. Mps1 phosphorylation sites regulate the function of Centrin 2 in centriole assembly. *Mol Biol Cell*. 2010;21:4361–4372.
25. Dantas TJ, Daly OM, Conroy PC, et al. Calcium-binding capacity of centrin2 is required for linear POC5 assembly but not for nucleotide excision repair. *PloS one*. 2013;8:e68487.
26. Sawant DB, Majumder S, Perkins JL, Yang CH, Eyers PA, Fisk HA. Centrin 3 is an inhibitor of centrosomal Mps1 and antagonizes centrin 2 function. *Mol Biol Cell*. 2015;26:3741–3753.
27. Liu X, Winey M. The MPS1 family of protein kinases. *Ann Rev Biochem*. 2012;81:561–585.
28. Musacchio A, Salmon ED. The spindle-assembly checkpoint in space and time. *Nat Rev Mol Cell Biol*. 2007;8:379–393.
29. Funabiki H, Wynne DJ. Making an effective switch at the kinetochore by phosphorylation and dephosphorylation. *Chromosoma*. 2013;122:135–158.
30. Janssen A, Kops GJ, Medema RH. Elevating the frequency of chromosome mis-segregation as a strategy to kill tumor cells. *P Natl Acad Sci USA*. 2009;106:19108–19113.
31. Janssen A, Kops GJ, Medema RH. Targeting the mitotic checkpoint to kill tumor cells. *Horm Canc*. 2011;2:113–116.
32. Hewitt L, Tighe A, Santaguida S, et al. Sustained Mps1 activity is required in mitosis to recruit O-Mad2 to the Mad1-C-Mad2 core complex. *J Cell Biol*. 2010;190:25–34.
33. Kwiatkowski N, Jelluma N, Filippakopoulos P, et al. Small-molecule kinase inhibitors provide insight into Mps1 cell cycle function. *Nature Chem Biol*. 2010;6:359–368.
34. Santaguida S, Tighe A, D'Alise AM, Taylor SS, Musacchio A. Dissecting the role of MPS1 in chromosome biorientation and the spindle checkpoint through the small molecule inhibitor reversine. *J Cell Biol*. 2010;190:73–87.
35. Tardif KD, Rogers A, Cassiano J, et al. Characterization of the cellular and antitumor effects of MPI-0479605, a small-molecule inhibitor of the mitotic kinase Mps1. *Mol Cancer Ther*. 2011;10:2267–2275.
36. Tannous BA, Kerami M, Van der Stoop PM, et al. Effects of the selective MPS1 inhibitor MPS1-IN-3 on glioblastoma sensitivity to antimitotic drugs. *J Natl Cancer Inst*. 2013;105:1322–1331.
37. Naud S, Westwood IM, Faisal A, et al. Structure-based design of orally bioavailable 1H-pyrrolo[3,2-c]pyridine inhibitors of mitotic kinase monopolar spindle 1 (MPS1). *J Med Chem*. 2013;56:10045–10065.
38. Wengner AM, Siemeister G, Koppitz M, et al. Novel Mps1 kinase inhibitors with potent antitumor activity. *Mol Cancer Ther*. 2016;15:583–592.
39. D'Alise AM, Amabile G, Iovino M, et al. Reversine, a novel Aurora kinases inhibitor, inhibits colony formation of human acute myeloid leukemia cells. *Mol Cancer Ther*. 2008;7:1140–1149.
40. Chen Z, Venkatesan AM, Dehnhardt CM, et al. Synthesis and SAR of novel 4-morpholinopyrrolopyrimidine derivatives as potent phosphatidylinositol 3-kinase inhibitors. *J Med Chem*. 2010;53:3169–3182.
41. Tumkevicius S, Dodonova J, Kazlauskas K, Masevicius V, Skardziute L, Jursenas S. Synthesis and photophysical properties of oligoarylenes with a pyrrolo[2,3-d]pyrimidine core. *Tetrahedron Lett*. 2010;51:3902–3906.
42. Vijay Kumar D, Hoarau C, Bursavich M, et al. Lead optimization of purine based orally bioavailable Mps1 (TTK) inhibitors. *Bioorg Med Chem Lett*. 2012;22:4377–4385.
43. Myrie KA, Percy MJ, Azim JN, Neeley CK, Petty EM. Mutation and expression analysis of human BUB1 and BUB1B in aneuploid breast cancer cell lines. *Cancer Lett*. 2000;152:193–199.
44. Yuan B, Xu Y, Woo JH, et al. Increased expression of mitotic checkpoint genes in breast cancer cells with chromosomal instability. *Clin Cancer Res*. 2006;12:405–410.
45. Jemaa M, Galluzzi L, Kepp O, et al. Characterization of novel MPS1 inhibitors with preclinical anticancer activity. *Cell Death Diff*. 2013;20:1532–1545.
46. Colombo R, Caldarelli M, Mennecozzi M, et al. Targeting the mitotic checkpoint for cancer therapy with NMS-P715, an inhibitor of MPS1 kinase. *Cancer Res*. 2010;70:10255–10264.
47. Mason JM, Lin DC, Wei X, et al. Functional characterization of CFI-400945, a Polo-like kinase 4 inhibitor, as a potential anticancer agent. *Cancer Cell*. 2014;26:163–176.
48. Morris GM, Goodsell DS, Halliday RS, et al. Automated docking using a Lamarckian genetic algorithm and an empirical binding free energy function. *J Comput Chem*. 1998;19:1639–1662.
49. Huey R, Morris GM, Olson AJ, Goodsell DS. A semiempirical free energy force field with charge-based desolvation. *J Comput Chem*. 2007;28:1145–1152.
50. Gasteiger J, Marsili M. Iterative partial equalization of orbital electronegativity – a rapid access to atomic charges. *Tetrahedron*. 1980;36:3219–3228.
51. Brueggemeier RW, Diaz-Cruz ES, Li PK, Sugimoto Y, Lin YC, Shapiro CL. Translational studies on aromatase, cyclooxygenases, and enzyme inhibitors in breast cancer. *J Ster Biochem Mol Biol*. 2005;95:129–136.
52. Diaz-Cruz ES, Shapiro CL, Brueggemeier RW. Cyclooxygenase inhibitors suppress aromatase expression and activity in breast cancer cells. *J Clin Endocrinol Metab*. 2005;90:2563–2570.
53. Majumder S, Fisk HA. VDAC3 and Mps1 negatively regulate ciliogenesis. *Cell Cycle*. 2013;12:849–858.
54. Liu C, van Dyk D, Choe V, et al. Ubiquitin ligase Ufd2 is required for efficient degradation of Mps1 kinase. *J Biol Chem*. 2011;286:43660–43667.